Joint Special Interest Group meeting between euspen and ASPE
Advancing Precision in Additive Manufacturing
Ecole Centrale de Nantes, France, September 2019
www.euspen.eu

Improving the dimensional accuracy of downfacing surfaces of additively manufactured parts

Umberto Paggi[1,2,3], Mirko Sinico[1,3], Lore Thijs[2], Wim Dewulf[1], Brecht van Hooreweder[1,3]

[1] *Department of Mechanical Engineering, KU Leuven, 3001 Leuven, Belgium*
[2] *3D Systems Leuven, 3001 Leuven, Belgium*
[3] *Member of Flanders Make - Core lab PMA-P, KU Leuven, 3001 Leuven, Belgium*

umberto.paggi@3dsystems.com

Abstract

In this study the accuracy of downfacing surfaces of small LPBF (Laser Powder Bed Fusion) fabricated features is investigated. Calibration geometries with downfacing angles ranging from 75° to 25° are printed in three different layer thicknesses to quantify the dimensional error due to dross formation and other melt pool phenomena in the downfacing area. Their dimension is measured with a digital microscope and compared with the CAD model: all geometries show a negative mismatch which is proportional to the downfacing angle, therefore a correction parameter is calculated. To validate the effectiveness of this offset, microchannels with diameter ranging from 1 mm to 0.6 mm were printed both with and without the correction. Their deviations from the nominal diameter were investigated through the use of micro Computed Tomography. Results show less deviation from the nominal cylindrical CAD when the offset is applied, while the dross formation remains almost unaffected.

Laser Powder Bed Fusion, Downfacing surfaces, Beam Compensation, Microchannel accuracy, X-ray micro Computed Tomography

1. Introduction

The Laser Powder Bed Fusion technology has experienced a constant increase in popularity in recent years thanks to the possibility of producing near net shape components with a high degree of complexity which would be unattainable with standard manufacturing techniques.

Nonetheless, metal 3D printing still faces challenges in term of accuracy and surface quality. Downfacing surfaces, for example, are among the most common and most problematic features in the LPBF process. Typically, these areas suffer from localised overheating which produces drosses that negatively affect the surface roughness [1,2]. Furthermore, their geometrical accuracy is lower, compared to a middle section, because of warping and distortions that can happen on unsupported and overhanging areas [3,4,5]. This can be a major problem in complex geometries with unreachable downfacing regions because the dimensional error can be larger than the tolerances required and can lead to build failure [6,7,8].

To mitigate these problems the most common approach is to separate the sample in two zones, namely the middle zone which stands over the bulk metal of the previous layer and the downfacing zone which is printed directly above lose powder [9]. For each region the process parameters can be tuned in order to achieve the required properties (minimum density, low residual stresses, high surface quality and so on); in particular for the downfacing area a more stable weld track is generally desired [10,11,12].

Another approach which is typically followed in the industrial environment is to develop offsets and compensation parameters to balance all the aforementioned distortions. One main issue with the current procedures is that the same optimization is applied indiscriminately to downfacing surfaces with different angles, or at best a distinction is made between flat or almost flat overhangs (0° to ~20°) and generally sloped areas. This study investigates the possibility of developing correction factors which evolve gradually with the downfacing angle in order to reduce the amount of critical areas and therefore increase the freedom in the design and production phases.

To do so, calibration geometries are printed with a downfacing angle that varies from 75° to 25°. The offsets are calculated by measuring the difference between the samples' nominal width and the real width. To validate these results microchannels are produced both with and without the compensation factor. The channels are then analysed with an industrial microfocus CT (µ-CT) and the dimensional error reduction is estimated.

2. Materials and methods

2.1. Benchmarks design and manufacturing

In this study a series of calibration samples are produced to evaluate the dimensional deviation at different angles due to the downfacing region. The geometries are first designed with 3DXpert software provided by 3D Systems. This software

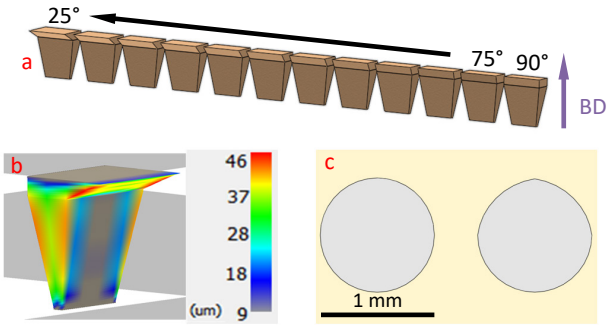

Figure 1. a) Calibration geometries with downfacing angle ranging from 75° to 25°; b) print simulation of the 25° sample; c) cross section of 1 mm microchannel without compensations (left) and with the offsets applied (right).

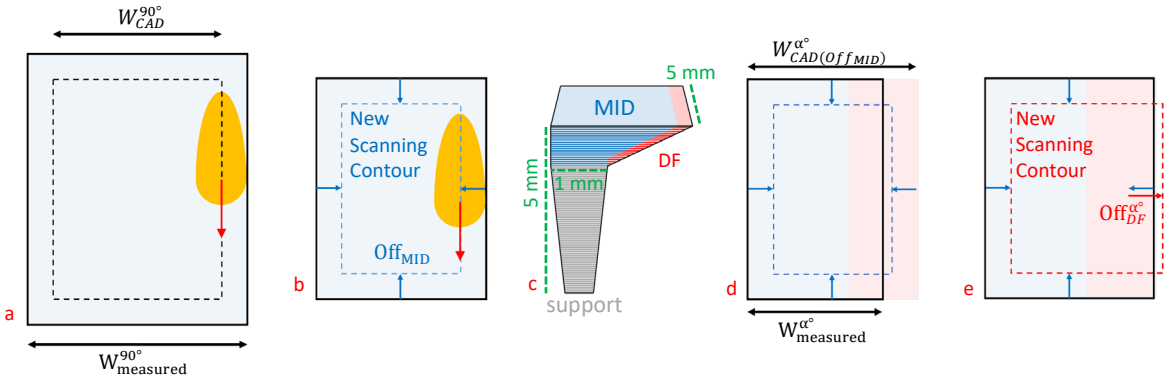

Figure 2. a) Sample printed without any correction; b) sample printed with middle offset; c) schematic of a general downfacing calibration sample; d) downfacing sample printed only with middle offset; e) downfacing sample printed with middle and downfacing offset.

includes a print simulation tool that estimates the distortion caused by shrinkage phenomena and residual stresses after the build (Figure 1b, note that it tends to overestimate the deviation magnitude). In order to account only for the error due to the localized effects proper of the downfacing region this tool has been used to create a CAD model which minimize the aforementioned distortions, typically linked to the sample's bulk.

Samples angles varying from 75° to 25° plus a reference at 90° (shown in Figure 1a) are printed in 30 µm, 60 µm and 90 µm layer thickness with a DMP Flex 350 in titanium powder LaserForm Ti Gr23 (A). To test the effectiveness of the correction parameter horizontal channels are also produced in 30 µm layer thickness. A cube of 10x10x10 mm was printed with two series of cylindrical holes of 1 mm, 0.8 mm and 0.6 mm diameter, one compensated and one not compensated. These features are selected because their dimension is in the same order of magnitude of the offsets, and therefore will benefit the most from this correction procedure. Likewise, the layer thickness is set at 30 µm because it grants the higher accuracy for small geometries and reduce the noise in the subsequent measures due to the surface roughness.

The initial calibration samples are lightly sandblasted to remove the sintered powder on the surface which would otherwise introduce high noise rending the data unreliable.

2.2. Samples analysis

The top surface of the calibration geometries is measured with a Keyence VHX-6000 digital microscope, using a 100x magnification. To avoid any operator dependency in the final value the width of the sample is calculated by interpolating the sample's sides with two parallel lines using the edge detection tool available in the microscope software. For each point four samples are measured and the standard deviation of these data is used as an estimation of the error.

To calculate the correction factors for different angles we compare the measured and nominal width of the calibration geometries' top surface. From these measurements two different offsets are derived: the first one is proper of the middle areas and is correlated to the error due the melt pool width. As shown in Figure 2a, if no correction is applied then the laser will scan the CAD contour and because of the melt pool dimension the final cross section will be bigger than the CAD one. Therefore, a middle offset is calculated as shown below and a new scanning contour is created (Figure 2b) so that the final dimension matches the 3D model.

$$\mathrm{Off_{MID}} = \left(W^{90°}_{CAD} - \mathrm{W^{90°}_{measured}}\right)/2$$

Where $\mathrm{Off_{MID}}$ is the correction factor for a middle region, $W^{90°}_{CAD}$ is the nominal width of the sample and $\mathrm{W^{90°}_{measured}}$ is the real width of the sample.

When a downfacing region is printed the compensation for the melt pool width is still applied, but other phenomena (explained below) affect the final cross section dimension (Figure 2d). Therefore, a new downfacing offset is calculated (Figure 2e), which is zero for a 90° sample since no downfacing area is present, and calculated as follow.

$$\mathrm{Off^{\alpha°}_{DF}} = W^{\alpha°}_{CAD(Off_{MID})} - \mathrm{W^{\alpha°}_{measured}}$$

Where $\mathrm{Off^{\alpha°}_{DF}}$ is the correction factor for a general downfacing region at an angle of α°, $W^{\alpha°}_{CAD(Off_{MID})}$ is the nominal width of the sample with the applied middle offset and $\mathrm{W^{\alpha°}_{measured}}$ is the real width of the sample.

Regarding the microchannels benchmark, this was analysed trough a µ-CT scan performed on a Nikon XTH 225ST machine at 195 kV, 62 µA, exposure 2000 ms, and tungsten target. A copper filter of 0.5 mm was used during the scan to reduce the beam hardening artefact. In total, 3142 projections were acquired at a magnification of ~20 and reconstructed with a voxel size of

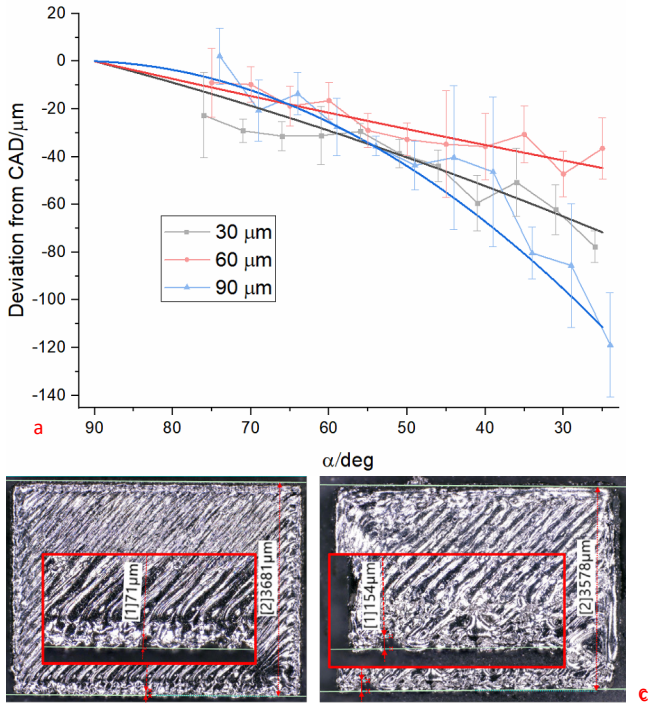

Figure 3. a) Downfacing geometry graph that shows the trend of the negative mismatch with the printed angle. b) 30° 30 µm layer thickness sample with detail of maximum deviation on the edge. c) 30° 90 µm layer thickness sample with detail of maximum deviation on the edge.

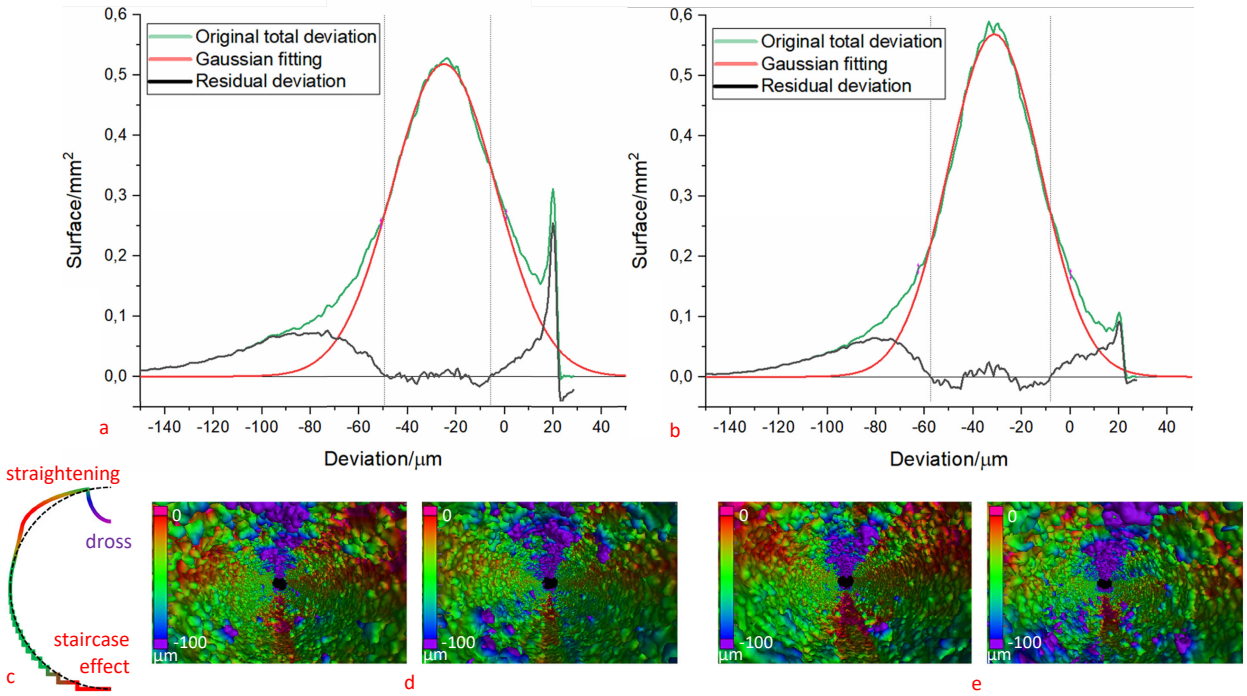

Figure 4. a) Deviation plot of the non-compensated 1 mm channel; b) deviation plot of the compensated 1 mm channel; c) schematic representation of the different deviations in a microchannel. CT scan of microchannels of d) 1 mm and e) 0.6 mm, compensated one on the right.

10 µm. The collected CT projections after reconstruction were imported in VGSTUDIO MAX 3.2.3. The mentioned software was used to first determine the surface of the acquired dataset, using an advanced ISO50% surface determination with a set searching distance of 40 µm. Subsequently, nominal cylinders of 1 mm, 0.8 mm and 0.6 mm were fitted against the compensated and non-compensated channels present in the benchmark. To avoid fitting errors, a first raw fit was performed with a manual alignment of the nominal cylinders followed by a refined best-fit executed with the advance refinement VGSTUDIO algorithm. A nominal/actual comparison was extrapolated comparing the nominal cylinders to the printed micro-channels, and a total of 6 deviation plots were exported (3 compensated and 3 non-compensated sets).

3. Results and discussion

3.1. Downfacing offset

The results for 30 µm, 60 µm and 90 µm layer thicknesses are shown in Figure 3a. A clear trend is shared between the three series which links larger downfacing angles to larger negative deviations.

This could be explained with the mechanism of fluid flow that occurs on melt pools supported mostly by the metal particles, as shown by Chen et al. [13]. The liquid metal is subject to a number of factors (capillarity forces, gravity, Marangoni convection flow and others) which create an unstable melt pool that sinks in the powder bed, reducing the final width of the scan track. Moreover, as reported by Wang et al. [5], the unsupported edges of the scan tracks are prone to bending upwards due to residual stresses, which leads to a negative deviation of the final shape in the x-y plane.

It is also clear that a thicker layer is correlated to a larger error. This is because larger melt pools are more instable and capillary forces make the melt track prone to break into spherical agglomerates [13]. The resulting rough edge has a maximum deviation comparable with the offset calculated for the corresponding angle, as shown in Figure 3c.

In order to have a more consistent offset which smoothly transitions from zero to the maximum measured deviation, the experimental data is fitted with a polynomial fit of grade 2, fixing a value of zero at 90° as explained above. This choice is arbitrary and does not represent any theoretical prediction of the melt pool behaviour, but it's still selected because it's quick to perform and because the resulting curves are within the error bars of almost all the data point. A linear fit was also tested but in this case the R-squared values are higher compared to the parabolic fit.

3.2. Compensation for microchannels

In microchannels two types of dimensional error can be typically identified [7]: at angles close to flat overhangs overheating and dross formation occurs, while from 90° to ~30° we see a straightening of the side of the cylinder which leads to a more squared cross section. As shown in Figure 4c, in the first case the cross section of the printed cylinder will be smaller than the desired dimension, therefore dross defects will be referred to as negative deviation. On the contrary, the squared shape resulting from the straightening is bigger than the cylindrical one and will be referred to as positive deviation.

In Figure 4d-e it's possible to identify these features both in the non-compensated and compensated channels. The negative deviations (in purple) are mainly due to dross and in some cases high surface roughness, whereas the positive deviations (in red) consist of the straightening effect on the downfacing region and the staircase effect on the bottom of the cylinder. Qualitatively, it's already possible to say that the downfacing offset plays a major role in smaller channels while the 1 mm cylinder still shows a relevant amount of straightening in the compensated geometry.

In Figure 4a a more detailed representation of the surface is given in the deviation plot .The main peak in the centre of the graph corresponds to the cylindrical surface, shown in green in Figure 4d-e. If the microchannel were perfectly round, smooth and equal to the CAD dimension, then on the graph there would be only a single vertical line placed at x = 0. In reality, the sample

	1 mm	1 mm comp	0.8 mm	0.8 mm comp	0.6 mm	0.6 mm comp
%Pos. Dev.	21.8	14.7	27.2	21.9	27.3	22.6
%Neg. Dev.	7.3	5.7	13.0	1.3	9.5	1.3

Table 1. Normalized area affected by positive and negative deviations. The nominal area employed for 1 mm, 0.8 mm and 0.6 diameter is respectively 31.4 mm^2, 25.12 mm^2, and 18.84 mm^2.

has a rough surface which deviates both in positive and negative direction and causes the values to spread. Following Schmähling and Hamprecht [14], this spread is assumed to be randomly distributed and therefore the peak can be interpolated with a Gaussian fit. Moreover, the centre of the peak is not at zero but is always shifted between -20 µm and -40 µm, which means that the diameter of the printed channel is smaller than the nominal one. These numbers are consistent with the thickness of the sintered powder layer that cannot be removed from internal features via sandblasting, but shrinkage phenomena could also be contributing to the cross section reduction.

After removing the central peak from the data three main regions can be defined: on the left we have the negative deviation caused by the dross, in the middle we have the noise and residue from the Gaussian subtraction which will not be considered further, and on the right there is the positive deviation due to the straightening and staircase effects. It's important to mention that several fitting intervals were tested to assess the interpolation influence on the final data and the results showed very little variation. To evaluate the effectiveness of the offsets the total areas affected by the positive and negative deviations are calculated and normalized with the nominal channel surface from the CAD model. Results are shown in Table 1.

All samples show a reduction in the straightening effect although the compensation strategy seems to work best for small feature which dimension is comparable to the offset value. It's interesting to notice that the dross effect is also slightly reduced because by printing a rounder shape the overhanging area close to 0° is less compared to the squared cross section shown in Figure 4c.

5. Conclusions

In this paper, LPBF calibration geometries are printed in 30 µm, 60 µm and 90 µm layer thickness with a downfacing angle that varies from 75° to 25°. The middle and downfacing offsets are calculated by measuring the difference between the samples' nominal width and the real width. The experimental data are then interpolated with a parabolic fit to obtain a smooth transition between zero and the maximal deviation, which equals ~70 µm for the 30 µm layer thickness. To validate these results microchannels of 1 mm, 0.8 mm and 0.6 mm diameter are produced both with and without the compensation factor. The channels are then analysed with an industrial microfocus CT and a reduction in the straightening effect of, respectively, 1.6 %., 11.7 %, and 8.2 % is achieved. A small improvement is also obtained on the sag defect with a reduction of 7.1 %, 5.3 %, and 4.7 %. This is because the squared profile caused by the straightening has a larger overhanging area close to 0° compared to the cylindrical shape. Therefore, by printing a cross section closer to the CAD model this critical overhanging zone is reduced.

It's important to note that these final numbers should be considered more as qualitative results rather than absolute ones. A series of approximations has been applied to the data, starting from the CT measurement itself which has a limited achievable resolution and yet unknown uncertainty. Moreover, the Gaussian fitting of the analysed deviations for the roughness contribution is not a perfect representation of the actual surface and some residual deviation from the model is always present.

Nonetheless, a reduction in both positive and negative deviations is clearly seen in the compensated channels, therefore it can be concluded that applying a localized correction specific for every downfacing angle definitely improves the accuracy of small and fine features.

In future work a larger set of calibration samples should be measured to decrease the standard deviation on the single data points. Small geometries in 60 µm and 90 µm should also be printed to check the effectiveness of the downfacing offset for these parameters, but the accuracy of these two layer thicknesses is generally low and often leads to occlusions which render the microchannels non-functional. Therefore, some other types of benchmark should be designed. Finally, more attention should be given also to shrinkage and other phenomena that affect the build accuracy and that scale with the feature dimension, to understand why the offset strategy seems less effective on the 1 mm cylinder.

Acknowledgements

This research was funded by The EU Framework Programme for Research and Innovation - Horizon 2020 - Grant Agreement No 721383 within the PAM² research project.

References

[1] Jamshidinia, M. & Kovacevic, R. The influence of heat accumulation on the surface roughness in powder-bed additive manufacturing. Surf. Topogr.*: Metrol. Prop.* **3**, 014003 (2015).

[2] Xiang, Z., Wang, L., Yang, C., Yin, M. & Yin, G. Analysis of the quality of slope surface in selective laser melting process by simulation and experiments. *Optik* **176**, 68–77 (2019).

[3] Cheng, B. & Chou, K. Deformation Evaluation of Part Overhang Configurations in Electron Beam Additive Manufacturing. *Processing V001T02A072, ASME,* **Volume 1** (2015).

[4] Calignano, F. Design optimization of supports for overhanging structures in aluminum and titanium alloys by selective laser melting. *Materials & Design* **64**, 203–213 (2014).

[5] Wang, D., Yang, Y., Yi, Z. & Su, X. Research on the fabricating quality optimization of the overhanging surface in SLM process. *The International Journal of Advanced Manufacturing Technology* **65**, (2013).

[6] Pakkanen, J. et al. Study of Internal Channel Surface Roughnesses Manufactured by Selective Laser Melting in Aluminum and Titanium Alloys. *Metall and Mat Trans A* **47**, 3837–3844 (2016).

[7] Snyder, J. C., Stimpson, C. K., Thole, K. A. & Mongillo, D. J. Build Direction Effects on Microchannel Tolerance and Surface Roughness. *J. Mech. Des* **137**, 111411-111411–7 (2015).

[8] Atzeni, E. & Salmi, A. Study on unsupported overhangs of AlSi10Mg parts processed by Direct Metal Laser Sintering (DMLS). *Journal of Manufacturing Processes* **20**, 500–506 (2015).

[9] Cloots, M., Zumofen, L., Spierings, A. B., Kirchheim, A. & Wegener, K. Approaches to minimize overhang angles of SLM parts. *Rapid Prototyping Journal* **23**, 362–369 (2017).

[10] Charles, A. et al. Effect of process Parameters on Dimensional accuracy of Down-facing surfaces in Selective Laser Melting of Ti6Al4V. *ASPE and euspen Summer Topical Meeting - Lawrence Berkeley National Laboratory, Berkeley, California, USA* **Volume: 69***,* (2018)

[11] Fox, J. C., Moylan, S. P. & Lane, B. M. Effect of Process Parameters on the Surface Roughness of Overhanging Structures in Laser Powder Bed Fusion Additive Manufacturing. *Procedia CIRP* **45**, 131–134 (2016).

[12] Mertens, R., Clijsters, S., Kempen, K. & Kruth, J.-P. Optimization of Scan Strategies in Selective Laser Melting of Aluminum Parts With Downfacing Areas. *Journal of Manufacturing Science and Engineering* **136**, (2014).

[13] Chen, H., Gu, D., Xiong, J. & Xia, M. Improving additive manufacturing processability of hard-to-process overhanging structure by selective laser melting. *Journal of Materials Processing Technology* **250**, 99–108 (2017).

[14] Schmähling, J. & Hamprecht, F. A. Generalizing the Abbott–Firestone curve by two new surface descriptors. *Wear* **262**, 1360–1371 (2007).